ABRUPT ONSET OF LARGE SCALE NONPROTON ION RELEASE IN PURPLE MEMBRANES CAUSED BY INCREASING pH OR IONIC STRENGTH

TIM MARINETTI
The Rockefeller University, New York, New York 10021

ABSTRACT The abrupt onset of large scale nonproton ion release by photo-excited purple membrane suspensions has been observed near neutral pH using transient conductivity measurements. At pH 7 and low ionic strength, the conductivity transients due to proton and nonproton ions are of comparable magnitude but of opposite sign: fast proton release and ion uptake, followed by slow proton uptake and ion release. By increasing either the pH or the NaCl concentration, the amplitude of the conductivity transient increases sharply and the signal is then dominated by nonproton ion release. These results can be understood in terms of light-induced changes in the population of counterions condensed at the purple membrane surface caused by changes in the surface charge density. The critical charge density required for condensation to occur is evidently achieved near neutral pH by ionizing dissociable groups on the membrane by either titration (increasing the pH) or shifting their pKs (increasing the ionic strength).

INTRODUCTION

Bacteriorhodopsin (bR) is the single polypeptide component of the purple membrane (PM) of *Halobacterium halobium*, and functions as a light-driven proton pump (1). The structure and function of bR and the PM have been extensively reviewed (2–5).

Transient proton release and uptake by bR in response to actinic light flashes has been reported using indicator dyes (6–9), volume changes (10–12), and transient conductivity (13, 14). There is some controversy over the order of uptake and release at low pH. Mitchell and Rayfield (9) observe release before uptake at pH 4; our results (13) and those of other workers (8, 15) indicate the opposite, in consonance with steady-state measurements (16, 17). At neutral pH there is general agreement that proton release occurs before uptake.

The PM exhibits a net negative surface charge (18, 19), and substantial structural changes during the bR photoreaction cycle have been reported (20, 21). If such changes resulted in changes in the distribution or number of exposed surface charges, then ions other than protons could be transiently moved on and off the PM. This was suggested by Slifkin et al. (22, 23) to explain their light modulation conductivity experiments and was subsequently proven in our laboratory (13, 14) by direct observation of the conductivity transients. These latter experiments were done in low and very high ionic strengths, respectively.

Here, transient conductivity measurements were performed in the intermediate ionic strength region to study the onset of large scale nonproton ion movements. This occurs at low ionic strength (20 mM NaCl) by increasing the pH to 8, or at pH 7 by increasing the ionic strength to ~0.2 M. Below the transition, nonproton ion uptake occurs along with proton release. Above the transition, the flash-induced signals are dominated by nonproton ion release and the amplitude increases as the ionic strength is raised. These results will be interpreted in terms of ion condensation in polyelectrolyte systems, a process analyzed in detail by Manning (24) for linear polyions.

MATERIALS AND METHODS

The 100-kHz differential conductivity apparatus used to perform these experiments, as well as the calculations used to analyze the data, has been described previously (13, 14). Since those reports, a photodiode and associated circuitry has been added to monitor the actinic light intensity for each measurement.

H. halobium strain S-9 were grown from a slant kindly provided by Dr. W. Stoeckenius, and PM was prepared as described in Oesterhelt and Stoeckenius (25). Samples used for the conductivity measurements were briefly sonicated before use, after the PM was washed into the indicated starting buffers by several cycles of centrifugation and resuspension. The final optical absorbance at 570 nm was ~0.5 in a 1-cm cell, corresponding to a bR concentration of 8 μM.

EXPERIMENTAL RESULTS

Conductivity changes after an actinic flash are caused by both changes in the concentration of small mobile ions due to the photoreaction cycle of bR (e.g., binding or release) and the minute heating of the sample caused by the absorbed light. The former appears as a transient signal that rises and decays (convoluted with the 1-ms response time of the apparatus). The latter gives an apparent dc baseline shift because the conductivity of all ions increases with temperature, and thermal relaxation is slow compared with the time frame of observation. Transients due to

protons can be unambiguously distinguished from nonproton signals by variation of the composition of the buffer in the suspending electrolyte (13, 14). On the 1-ms timescale, equilibration of protons with the buffer ions is unobservably fast, so proton transients appear as changes in the concentrations of the buffering ions present, and these can be chosen to give either a positive or a negative sign depending on the net change in charge upon protonation, namely, acetate vs. ammonia. Variation of the buffer allows us to determine which component of the signal is due to protons, while the long-time baseline shift serves as an actinometer, proportional to the total light absorbed and the bulk conductivity of the sample. Thus, both the nature (proton vs. nonproton) and the quantum yield of the ions responsible for the conductivity transient can be determined independently.

The results of a pH titration of a sample starting in 2 mM tetramethylethylenediamine (TEMED), 20 mM NaCl at 17.0°C are shown in Fig. 1. The sharp spike in the first few milliseconds after the flash is due to an electrical artifact caused by the laser discharge and can be seen in the absence of bR. At the lower pHs, the rise time of the transient is limited by the 1-ms time resolution of the lock-in amplifier; the decay time (1/e) from a single exponential fit to the tail of the data is 15 ms between pH 6 and 7. At the higher pH end, the rise time is resolved and the data are well fit by a single exponential rise and a single exponential decay. For trace *G*, the time constants are 2.9 ± 0.1 ms and 39 ± 1 ms, respectively. Note that in all cases, regardless of the sign of the transient, the baseline after the transient signal decay is always shifted positive relative to that before the flash. This is the thermal heating effect discussed above.

In TEMED buffer (pK 5.9), and with the glycinamide added in trace *E* to maintain buffer capacity at the higher pHs, transients due to proton release should be positive since protonation of the buffer ions increases their net charge. Instead, a negative transient is observed, which decreases in absolute amplitude as the pH is raised. Above pH 7, the signal reverses sign and the amplitude increases quite sharply. In trace *H*, excess phosphate buffer is added. This should reverse the sign of the component of the transient due to protons, but the signal actually increases slightly. Hence at pH 8, most of the transient must be due to ions other than protons. The apparent increase in the signal amplitude in trace *H* compared with trace *G* could be due to the increases in the ionic strength of the sample (see below) since at pH 8 adding 12 mM phosphate is equivalent to adding ~45 mM NaCl. The data of Fig. 1 show clearly that nonproton ions are moving after the flash. At low pH they are evidently taken up by the PM before release, since the net transient represents a loss of conductivity, i.e., ion uptake. In alkaline solution, however, this reverses, and the yield of ions increases as well.

Fig. 2 shows the effect of varying first the buffer composition and then the ionic strength at pH 7 at 17.0°C. Traces *A–D* show clearly that a negative component in the transient grows in as low concentrations of phosphate are added. This is exactly as expected for fast proton release followed by slower uptake. This should have given a positive signal in trace *A* (in TEMED buffer alone), but almost no transient is observed. This could easily be

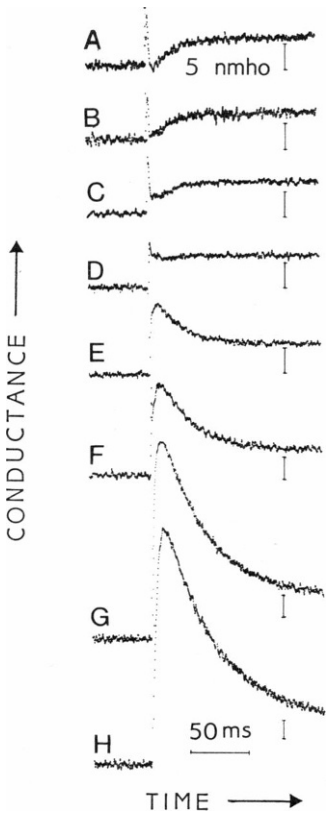

FIGURE 1 pH variation of light-induced conductivity transients in 20 mM NaCl. bR starts in 2 mM TEMED buffer pH 6.21 (*A*). pH is then adjusted with KOH and NaOH to 6.48 (*B*), 6.75 (*C*), and 6.95 (*D*). Then, 3 mM glycinamide was added, pH 7.4 (*E*) and the pH raised to 7.82 (*F*) and 8.1 (*G*). Finally, phosphate buffer was added (12.6 mM) and the pH adjusted to 8.1 (*H*). The vertical bar near the end of each trace is a change of 5 nmho; the sensitivity varies as the ionic strength of the sample changes. *C–F* are the average of 128 flashes; all others are 64.

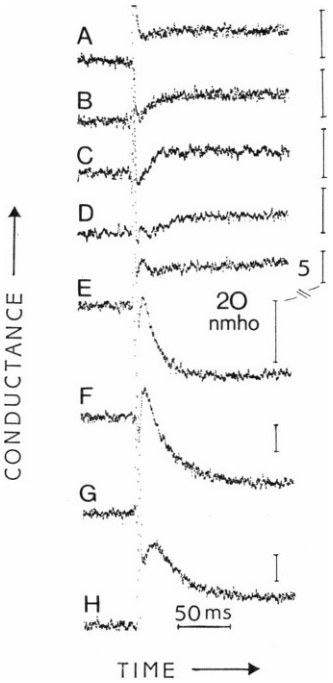

FIGURE 2 bR at pH 7: effect of buffer variation and ionic strength increase on light-induced conductivity transients. bR starts in 2 mM TEMED, 20 mM NaCl, pH 6.98 (*A*). Then phosphate is added to the following concentrations (mM) and pH: 0.3, 6.96 (*B*); 0.6, 6.97 (*C*); 1.9, 6.96 (*D*). Then NaCl is added to the following concentrations (mM) and pH: 51, 6.96 (*E*); 150, 6.98 (*F*); 500, 6.95 (*G*). Finally, phosphate is added to 11.4 mM, pH 6.9 (*H*). The vertical bar at the end of each trace gives the scale in nmho: note the change at trace *F* and beyond. All traces are the average of 128 flashes.

explained by an additional component of nonproton ion uptake occurring at the same time as the proton release, which would then give a net conductivity change near 0. Traces *E–G* show the effect of increasing the ionic strength with NaCl. There is a dramatic increase in the signal amplitude at trace *F*. Note that changing the ionic strength, and hence the bulk conductivity, alters the sensitivity of the conductivity bridge. This is reflected in the vertical bars by each trace which convert the observed signal voltage into absolute conductivity units. Clearly, a positive component grows in as the salt concentration is raised. Trace *H* shows the effect of adding excess phosphate buffer: there is a decrease in the signal amplitude. Part of this is due to a decrease in the measured laser power in this particular sample, but some of the decrease is due to the proton release component of the signal, which is now small compared with the nonproton component. These data show that increasing the ionic strength can cause the reversal of the nonproton ion transient from small and negative to large and positive, similar to the effect of increasing pH illustrated in Fig. 1

Fig. 3 gives the results of a buffer titration similar to the first part of Fig. 2, except performed at pH 6.2. The magnitude of the transient (in nmho) is plotted against the calculated equivalent conductance change (in mho cm^2/eq) for protonation of the different buffers. The titration starts in TEMED (point furthest to right) and proceeds to the left as phosphate is added. If the amount of protons and nonproton ions moving after the flash were independent of the buffer composition, the data should lie on a straight line since all that changes is the algebraic sign and magnitude of the proton component in the different buffers. With the exception of the center point, the data lie on a line within the indicated errors, taken from the amplitude of the noise in the traces. The intercept at $\Lambda = 0$, i.e., where the buffer composition is such that proton release by bR

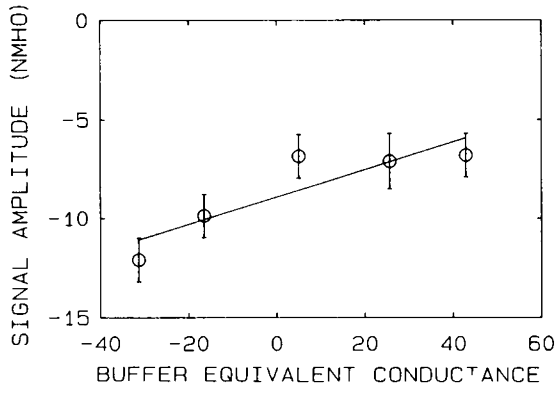

FIGURE 3 bR at pH 6.2: summary of buffer variation. The observed signal amplitude (in nmho) is plotted vs. the calculated equivalent conductance (in mho cm^2/eq) for protonation of each buffer mixture. The points go sequentially from right to left, beginning in 2 mM TEMED, 20 mM NaCl with the following phosphate concentrations (mM): 0, 0.6, 1.9, 5.1, and 11.3. Calculations were done as described in reference 14. The line is a least squares fit to the points.

produces no net conductivity change, gives the amplitude of the nonproton ion signal. If this were due to sodium ion, for example, comparing the nonproton amplitude to the calculated proton component and correcting for the difference in equivalent conductances, the result is that 2–3 Na^+ are taken up per proton released at this pH.

Using the ratio of the transient amplitude to the thermal baseline shift, the yields of the nonproton ions released at alkaline pH (Fig. 1) or at increased NaCl (Fig. 2) may be estimated. As we have shown (13, 14), the quantity that is directly observed is the product of the quantum yield times the equivalent conductance of the released ion. Although these measurements cannot identify which particular nonproton ion is responsible for the transient, reasonable bounds can be placed on the yields since the equivalent conductance for all typical small ions (except protons and hydroxide) is in the range of 30–70 mho cm^2/eq. Using sodium ($\Lambda = 45$) as an example, the sample of Fig. 1 *H* has a quantum yield of 1, and those of Fig. 2, *F–H* range from 2 to 8, increasing with the salt concentration. The pH 8 value is in excellent agreement with the value we reported earlier (13) for a sample at that pH and a similar ionic strength, although with different electrolytes. The high salt yields also approach those observed in 1 M NaCl (14). Note that these quantum yields are ions per photon absorbed; normalizing them to the amount of a particular photocycle intermediate such as M412 would only make the ion yields larger.

One possible objection can be raised in the use of TEMED as a buffer, since a recent report (26) claims that low concentrations of diamines reverse the direction of the proton pump. There are reasons to question these authors' interpretation of the electrical signals, particularly on the long timescales (>1 ms) relevant to the experiments presented here. Tóth-Boconádi et al. (26) report that the apparent reversal of the pump is itself reversed by either increasing the TEMED concentration, or by adding small amounts of Ca^{++} or larger amounts of Na^+. This in itself strongly suggests that the complex signals at long times are in fact due to charge movements in the interfacial region between the PM and the electrolyte and not inside the bR itself. It is interesting that the fast charge movements reported by Tóth-Boconádi et al. (26), which are due to charge displacements inside bR and presumably reflect the first steps of the pump, are not affected by TEMED. However, even if one accepts the interpretation of Tóth-Boconádi et al., the point is moot since the experiments reported here were done at much higher TEMED concentrations than are required to restore the "normal" direction of the proton pump.

To remove any ambiguity, the experiments of Figs. 1 and 2 were repeated using the monoamine imidazole as buffer instead of TEMED. No reversal of the proton movements was seen and the change from nonproton ion uptake to release caused by increasing pH or ionic strength was the same as with TEMED.

DISCUSSION

The transient conductivity measurements reported above can be most simply understood as resulting from two processes. First, there is the well-established rapid proton release followed by slower uptake in response to a light flash in the region near pH 7. This is clear from the changes in the signal amplitudes caused by variation of the buffer composition (Figs. 2 and 3). However, there is evidently another component in the transient since the signal amplitudes do not behave quantitatively as if the entire signal were due to protons only. This is clear from the samples with TEMED only (Figs. 1 *A* and 2 *A*) or imidazole (data not shown), buffers in which the signal should be positive but is observed to be negative. Also, the large positive transient does not become negative when phosphate is made the dominant buffer. Hence nonproton ions are transiently moving as well. The proton and nonproton movements evidently occur on the same timescale and with the same kinetic constants since single exponential decays (and where resolved, the rise as well) are observed.

The data presented herein show that the nonproton ion movements undergo a dramatic change near neutral pH. At low ionic strength and at pH <7, the nonproton ions are bound to the PM as the protons are released. Thus the observed conductivity signal is the sum of opposing transients with very similar or identical amplitudes. However, if the pH is raised to 8 or if the salt concentration is raised, the nonproton ion movements become much larger in magnitude, and their direction is reversed—they are released, then taken up. The yields of the ion transients approach values on the order of 10 ions per photon at high ionic strength, in agreement with previous results (14).

The PM has two sources of negatively charged groups: lipid phosphates and sulfates and protein carboxyl groups, some of which can have quite high effective pKs due to the large negative charge of the PM. In addition, a substantial portion of the PM lipid is phosphatidyl glycerol phosphate (27, 28), which carries more than one charge and should have a high pK. The electrostatic effects described below would affect these phosphate groups as well. It is well known from studies with polymers containing carboxylic acid side groups that the titration curves show a pK that depends on the degree of neutralization of the acids. The measured titration curves for poly(aspartic acid) (29), poly(acrylic acid) (30), poly(methacrylic acid) (31), and poly(L-glutamic acid) (32) all show quite broad buffering regions, and this pK range is lowered by 1–1.5 pH units as the ionic strength is raised. This is easily understood as screening of the closely spaced charges on the polymer, thereby reducing the electrostatic work needed to ionize further carboxyl groups. Manning (33) has analyzed the titration curve of a poly acid in terms of his ion condensation theory and finds a predicted lowering of the apparent pK as salt is added. The same is observed to occur in phosphatidylserine vesicles: the apparent pK is broad and shifts down from 6.0 in 1 mM NaCl to 3.7 in 1 M (34). Titrations of PM samples in different suspending NaCl concentrations exhibit a shift in a buffering region below neutral pH as the salt is raised (data not shown).

Manning's theory (see reference 24 and references therein) for linear polyions indicates that when the spacing between the charges on the polyion becomes comparable or less than the Bjerrum length (i.e., the distance at which the electrostatic interaction between two single charges is equal to kT; in water at 25°C this is 7.1 Å), then counterions condense on the polyion to screen a fraction of the charge. By condensed, Manning (35) refers to ion territorially confined to a small region in the vicinity of the polyion. In terms of the experiments here, such condensed counterions doe not contribute to the bulk conductivity—they move with the polyion and effectively reduce its net charge. Qualitatively similar results as those of Manning were obtained by two groups (36, 37) who obtained analytical and numerical solutions to the Poisson–Boltzmann equation. In particular, the latter group (37) investigated the effect of the geometry of the polyion on the counterion distribution. In the case of the plane, which is obviously closer to the PM than the cylindrical case normally considered, Gueron and Weisbuch (37) found that there is a critical surface charge density above which one observes high counterion concentrations near the surface, which are only slightly affected by ionic strength. This density (in e/nm^2) is $1/(2\pi z l_B \lambda)$, where z is the counterion valence, l_B is the Bjerrum length, and λ is the Debye length (the reciprocal of the Debye screening parameter κ). At 100 mM univalent salt or less, this means that the surface charge density must be $>0.22\ e/nm^2$.

A simple explanation of the abrupt onset of ion release is that in low salt and at pH <7, a sufficient fraction of the carboxyl side chains is not ionized, so that the net charge density is below the critical value. By increasing the pH or by increasing the ionic strength at pH 7, more of the carboxyl groups ionize and the net charge density rises above the critical value. During the photocycle, conformational changes cause changes in the distribution of the exposed surface charges and hence changes in the population of condensed counterions. Gueron and Weisbuch (37) report that above the critical charge density, the counterion concentration in the vicinity of the polyion (what they call the CIV) is proportional to the square of the charge density. If the charge density goes below the critical value, a significant portion of the accumulated counterions would be transiently released into the bulk phase. This would explain the large nonproton signal observed. The much smaller nonproton ion uptake can be understood by the fact that release of a proton must necessarily increase the negative charge on the PM. If the overall charge density of the PM surface is less than critical—evidently this is true at low salt and pH <7—no large scale changes in accumulated counterions is possible, but the negatively charged

group left after escape of the proton would be screened by some binding of positive ions.

To see if counterion condensation is a reasonable possibility, the charge density of the PM can be estimated from its known composition and structure (2). Kates et al. (27) report a total of 18 polar lipids per unit cell in PM, most of which are negatively charged, and this will add to the charge on the protein. From the model reproduced in reference 4, the maximum net negative charge due to the charged amino acids near the surface would be -5 per bR for the cytoplasmic side and ~ 0 for the extracellular side. The difference between the two sides estimated here (five charges) is close to that determined experimentally in measurements of the permanent electric dipole of bR before and after treatment with papain (38). If the lipids are distributed equally on either side of the membrane, then the maximum average charge densities are 0.88 and 0.5 e/nm^2, respectively, i.e., above or close to the critical density Gueron and Weisbuch found was required for counterion accumulation. This assumes all the lipid phosphates carry their maximum negative charge. If not all of the carboxyl and phosphate groups were ionized, then the surface charge density would be less.

The lipids may not be evenly distributed. Henderson et al. (39) present evidence from electron microscopy that the glycolipid is concentrated on the extracellular side of the PM. Using fluorescence quenching of specifically dansylated PM by uranyl ion, Renthal and Cha (40) inferred that the lipid phosphate is mostly on the cytoplasmic side. If one redistributes the lipids with these experiments taken into account, the effect is to make the cytoplasmic side more negative (maximum charge density ~ 1 e/nm^2) with a corresponding reduction in the charge on the extracellular side (drops to 0.35 e/nm^2). Again, this is an estimate of the maximum charge density, assuming all carboxyl and phosphate groups are ionized. These charge densities are very close to those calculated by Renthal and Cha (40) based solely on the phospholipids but assuming a larger lipid content per unit cell.

The charged lipids contribute significantly to the surface charge density due to the protein alone, shifting the total closer to the critical value, where it can be modulated by changes in the exposure or charge state of the PM carboxyl groups. The change in accumulated counterions due to changes in the surface charge density, i.e., the derivative of the CIV as a function of charge density, will determine the size of the light-induced conductivity transient. Qualitatively, it is clear that the surface charge density of the PM must be near the critical value for ion condensation since at densities either much lower or much higher, the fraction of counterions condensed is insensitive to changes in surface charge. Here it should be noted that polyelectrolyte systems often display highly nonlinear behavior as the net charge is varied. In the extreme case, one observes abrupt changes in physical properties, indicative of a molecular phase transition. An example is the ionic strength dependence of the diffusion coefficient of sodium poly(styrene sulfonate) (41), which changes by orders of magnitude at critical salt concentrations, depending on the valence of the counterion.

Light-induced changes in the surface potential of the PM have been reported by a variety of probe techniques, and the reader is referred to the discussion section of our previous paper (14) for a summary of that work. Conformational changes in bR during the photocyle have also been reported, e.g., molecular rotations (21) and helix tilting (20). The latter is still controversial: a recent Fourier transform infrared study (42) disputes the possibility of extensive helix tilt in the M412 intermediate. Also, optical dichroism experiments (43) show no significant changes in the angle of the chromophore's transition dipole in the early stages of the photocycle, and the difference Fourier between bR and M412 trapped at low temperature indicates no large scale protein movement (44). However, both of these reports explicitly state that there is no contradiction between their results and the molecular rotations seen by Ahl and Cone (21), since the studies in references 43 and 44 are on timescales and at temperatures, respectively, where the rotations might not be observed. It is noteworthy that time-resolved x-ray experiments record disorder in photostimulated bR films (45).

The data reported here strongly indicate some alteration in the surface charge distribution of the PM during the photocycle. This could be due to molecular rotations, but it is equally possible that other movements, such as displacements of the helices normal to the plane of the membrane, could be responsible. Such motions would certainly alter the positions of charged groups (46) and consequently alter the distribution of condensed counterions, but would not be detected in the optical or electron diffraction experiments.

These experiments, of course, do not distinguish between the two sides of the PM, which evidently are asymmetric (39, 40). Studies with oriented samples should help us to determine if there is side specificity to the counterion accumulation and the light-induced nonproton ion release, and experiments with liposomes are in progress.

I would like to acknowledge the excellent technical help of Irene Zielinski-Large who maintained the *H. halobium* cultures and prepared the PM. Dr. David Mauzerall contributed to discussions on the ion condensation problem. I would like to thank a referee for the helpful and clarifying comments.

This work was supported by National Institutes of Health grant GM32955-02.

Received for publication 18 September 1986 and in final form 26 January 1987.

REFERENCES

1. Oesterhelt, D., and W. Stoeckenius. 1973. Functions of a new photoreceptor membrane. *Proc. Natl. Acad. Sci. USA.* 70:2853–2857.

2. Henderson, R. 1977. The purple membrane from *Halobacterium halobium*. *Annu. Rev. Biophys. Bioeng.* 6:87–109.
3. Stoeckenius, W., R. Lozier, and R. A. Bogomolni. 1979. Bacteriorhodopsin and the purple membrane of *Halobacteria*. *Biochim. Biophys. Acta.* 505:215–278.
4. Stoeckenius, W., and R. A. Bogomolni. 1982. Bacteriorhodopsin and related pigments of *Halobacteria*. *Annu. Rev. Biochem.* 52:587–616.
5. Dencher, N. A. 1983. The five retinal-protein pigments of halobacteria: bacteriorhodopsin, halorhodopsin, P565, P370 and slow-cycling rhodopsin. *Photochem. Photobiol.* 38:753–767.
6. Lozier, R. H., W. Niederberger, R. A. Bogomolni, S.-B. Hwang, and W. Stoeckenius. 1976. Kinetics and stoichiometry of light-induced proton release and uptake from purple membrane fragments. *Halobacterium halobium* cell envelopes, and phospholipid vesicles containing oriented purple membrane. *Biochim. Biophys. Acta.* 440:545–556.
7. Govindjee, R., T. G. Ebrey, and A. R. Crofts. 1980. The quantum efficiency of proton pumping by the purple membrane of *Halobacterium halobium*. *Biophys. J.* 30:231–242.
8. Dencher, N. A., and M. Wilms. 1975. Flash photometric experiments on the photochemical cycle of bacteriorhodopsin. *Biophys. Struct. Mech.* 1:259–271.
9. Mitchell, D., and G. W. Rayfield. 1986. Order of proton uptake and release at low pH. *Biophys. J.* 49:563–566.
10. Ort, D. R., and W. W. Parson. 1978. Flash-induced volume changes of bacteriorhodopsin-containing membrane fragments and their relationship to proton movements and absorbance transients. *J. Biol. Chem.* 253:6158–6164.
11. Ort, D. R., and W. W. Parson. 1979. The quantum yield of flash-induced proton release by bacteriorhodopsin-containing membrane fragments. *Biophys. J.* 25:341–354.
12. Ort, D. R., and W. W. Parson. 1979. Enthalpy changes during the photochemical cycle of bacteriorhodopsin. *Biophys. J.* 25:355–364.
13. Marinetti, T., and D. Mauzerall. 1983. Absolute quantum yields and proof of proton and non proton transient release and uptake in photoexcited bacteriorhodopsin. *Proc. Natl. Acad. Sci. USA.* 80:178–180.
14. Marinetti, T., and D. Mauzerall. 1986. Large transient nonproton ion movements in purple membrane suspensions are abolished by solubilization in Triton X-100. *Biophys. J.* 50:405–415.
15. Bogomolni, R. A., W. Hubbell, and W. Stoeckenius. 1986. Cation binding changes during the bacteriorhodopsin photocycle. *Biophys. J.* 49(2, Pt. 2):212*a*. (Abstr.)
16. Garty, H., G. Klemperer, M. Eisenbach, and S. R. Caplan. 1977. The direction of light-induced pH changes in purple membrane suspensions. *FEBS (Fed. Eur. Biochem. Soc.) Lett.* 81:238–242.
17. Takeuchi, Y., K. Ohno, M. Yoshida, and K. Nagano. 1981. Light-induced proton dissociation and association in bacteriorhodopsin. *Photochem. Photobiol.* 33:587–592.
18. Fisher, K. A., K. Yanagimoto, and W. Stoeckenius. 1978. Oriented absorption of purple membrane to cationic surfaces. *J. Cell Biol.* 77:611–621.
19. Neugebauer, D. C., D. Oesterhelt, and H. P. Zingsheim. 1978. The two faces of the purple membrane. II. Differences in surface charge properties revealed by ferritin binding. *J. Mol. Biol.* 125:123–135.
20. Draheim, J. E., and J. Y. Cassim. 1985. Large scale global structural changes of the purple membrane during the photocycle. *Biophys. J.* 47:497–507.
21. Ahl, P. L., and R. A. Cone. 1984. Light activates rotations of bacteriorhodopsin in the purple membrane. *Biophys. J.* 45:1039–1049.
22. Slifkin, M. A., H. Garty, and S. R. Caplan. 1978. Modulation-excitation methods in the study of bacteriorhodopsin. *In* Energetics and Structure of Halophilic Microorganisms. S. R. Caplan and M. Ginzburg, editors. Elsevier/North-Holland Biomedical Press, Amsterdam. 165–184.
23. Slifkin, M. A., H. Garty, W. V. Sherman, M. F. P. Vincent, and S. R. Caplan. 1979. Light-induced conductivity changes in purple membrane suspensions. *Biophys. Struct. Mech.* 5:313–320.
24. Manning, G. S. 1978. The molecular theory of polyelectrolyte solutions with applications to the electrostatic properties of polynucleotides. *Quart. Rev. Biophys.* 11:179–246.
25. Oesterhelt, D., and W. Stoeckenius. 1974. Isolation of the cell membrane of *Halobacterium halobium* and its fractionation into red and purple membrane. *Methods Enzymol.* 31:667–678.
26. Tóth-Boconádi, R., S. G. Hristova, and L. Keszthelyi. 1986. Diamines reverse the direction on the bacteriorhodopsin proton pump. *FEBS (Fed. Eur. Biochem. Soc.) Lett.* 195:164–168.
27. Kates, M., S. C. Kushwaha, and G. D. Sprott. 1982. Lipids of purple membrane from extreme halophiles and of methanogenic bacteria. *Methods Enzymol.* 88:98–111.
28. Kushwaha, S. C., M. Kates, and W. Stoeckenius. 1976. Comparison of purple membrane from *Halobacterium cultirubrum* and *Halobacterium halobium*. *Biochim. Biophys. Acta.* 426:703–710.
29. McDiarmid, R., and P. Doty. 1966. The spectrophotometric titration of polyacrylic, poly-L-aspartic, and poly-L-glutamic acids. *J. Phys. Chem.* 70:2620–2627.
30. Mandel, M., and J. C. Leyte. 1962. A note on dissociation constants of poly carboxylic acids. *J. Polym. Sci.* 56:S25–S28.
31. Leyte, J. C., and M. Mandel. 1964. Potentiometric behavior of polymethacrylic acid. *J. Polym. Sci.* 2 (Part A):1879–1891.
32. Wada, A. 1960. Helix-coil transformation and titration curve of poly-L-glutamic acid. *Mol. Phys.* 3:409–416.
33. Manning, G. S. 1981. Limiting laws and counterion condensation in polyelectrolyte solutions. 6. Theory of the titration curve. *J. Phys. Chem.* 85:870–877.
34. MacDonald, R. C., S. A. Simon, and E. Baer. 1976. Ionic influences on the phase transition of dipalmitoylphosphatidyl serine. *Biochemistry.* 15:885–891.
35. Manning, G. S. 1984. Limiting laws and counterion condensation in polyelectrolyte solutions. 8. Mixtures of counterions, species selectivitiy, and valence selectivity. *J. Phys. Chem.* 88:6654–6661.
36. LeBret, M., and H. Zimm. 1984. Distribution of counterions around a cylindrical polyelectrolyte and Manning's condensation theory. *Biopolymers.* 23:287–312.
37. Gueron, M., and G. Weisbuch. 1980. Polyelectrolyte theory. I. Accumulation, site-binding, and their insensitivity to polyelectrolyte shape in solutions containing finite salt concentrations. *Biopolymers.* 19:353–382.
38. Utomo, J., K. Ohno, Y. Takeuchi, and A. Ikegami. 1986. Surface charge movements of purple membrane during light adaptation. *Biophys. J.* 50:205–211.
39. Henderson, R., J. S. Jubb, and S. Whytock. 1978. Specific labeling of the protein and lipid on the extracellular surface of purple membrane. *J. Mol. Biol.* 123:259–274.
40. Renthal, R., and C.-H. Cha. 1984. Charge asymmetry of the purple membrane measured by uranyl quenching of dansyl fluorescence. *Biophys. J.* 45:1001–1006.
41. Drifford, M., and J.-P. Dalbiez. 1985. Effect of salt on sodium polystyrene sulfonate measured by light scattering. *Biopolymers.* 24:1501–1514.
42. Nabedryk, E., and J. Breton. 1986. Polarized Fourier transform infrared (FTIR) difference spectroscopy of the M_{412} intermediate in the bacteriorhodopsin photocycle. *FEBS (Fed. Eur. Biochem. Soc.) Lett.* 202:356–360.
43. Nagle, J. F., S. M. Bhattacharjee, L. A. Parodi, and R. H. Lozier.

1983. Effect of photoselection upon saturation and the dichroic ratio in flash experiments upon effectively immobilized systems. *Photochem. Photobiol.* 38:331–339.

44. Glaeser, R. M., J. Baldwin, T. A. Ceska, and R. Henderson. 1986. Electron diffraction analysis of the M_{412} intermediate of bacteriorhodopsin. *Biophys. J.* 50:913–920.

45. Frankel, R. D., and J. M. Forsyth. 1985. Time-resolved x-ray diffraction study of photostimulated purple membrane. *Biophys. J.* 47:387–383.

46. Raudino, A., and D. C. Mauzerall. 1986. The effect of local geometry on ion binding to proteins. *Biophys. J.* 49(2, Pt. 2):492*a*. (Abstr.)